Acta Crystallographica Section B
Structural Science
ISSN 0108-7681

New model for the hydroxyapatite–octacalcium phosphate interface

M. E. Fernández,[a] C. Zorrilla-Cangas,[b] R. García-García,[b] J. A. Ascencio[c] and J. Reyes-Gasga[b]*

[a]Instituto Nacional de Investigaciones Nucleares, Km 36.5 Carretera México-Toluca, Ocoyoacac Edo. de México 52045, Mexico, [b]Instituto de Física, UNAM, Circuito de la Investigación Científica s/n, Cd Universitaria, Coyoacán 04510 México DF, Mexico, and [c]Instituto Mexicano del Petróleo, Programa de Investigación y Desarrollo de Ductos, Eje Central Lázaro Cárdenas No. 152 Col San Bartolo Atepehuacan, CP 07730 México DF, Mexico

Correspondence e-mail: jreyes@fisica.unam.mx

Received 27 August 2002
Accepted 24 January 2003

Some experimental results have indicated that hydroxyapatite (HA) and octacalcium phosphate (OCP) can form an epitaxic interface. Subsequently the OCP–HA interface has become of great biological interest in the context of mineralized tissue formation. In this work a new OCP–HA interface model based on Brown's proposed configuration [Brown (1962), *Nature*, **197**, 1048–1050] and using the minimum interface free-energy optimization is presented. This new model is formed by half a unit cell of HA and one unit cell of OCP, as in Brown's model, but in our case $[1\bar{2}10]$ of HA is 'glued' with [010] of OCP. Therefore, the relationship found was: $[000\bar{1}]_{HA}$ parallel to $[001]_{OCP}$ and $[1\bar{2}10]_{HA}$ parallel to $[010]_{OCP}$. Self-consistent field methods were used for the analysis of Brown's model and ours. It is shown that the atoms in our model have similar environments as in the HA and OCP unit cells and that, as a result of the differences between HA and OCP unit-cell parameters, this interface presents misfit-dislocation-like features. High-resolution transmission electron microscopy (HREM) simulated images for the new interface model have been included and, when they are compared with the experimental ones, the similarity is quite good.

1. Introduction

Many experimental results (see *e.g.* Rooji & Nancollas, 1984; Nelson *et al.*, 1986; Miake *et al.*, 1990; Ijima, Tohda & Moriwaki, 1992; Ijima, Tohda, Suzuki *et al.*, 1992; Iijima & Moriwaki, 1998, 1999; Mathew & Takagi, 2001) have indicated that hydroxyapatite (HA) and octacalcium phosphate (OCP) can form a smooth epitaxic interface with a minimum of interfacial energy. In fact, OCP is considered thermodynamically to be a metastable phase of HA and crystallizes more rapidly in the platy habit (Iijima & Moriwaki, 1999). Thus, OCP was proposed to be the initial precipitate that transforms into an apatite by hydrolysis and plays a role as a template of epitaxic overgrowth of HAP (Ijima, Tohda, Suzuki *et al.*, 1992; Miake *et al.*, 1993). *In vitro* studies have shown that HA is able to grow epitaxically on the (100) surface of OCP in such a way that the *c* axes of HA and OCP are parallel to each other (Rooji & Nancollas, 1984; Nelson *et al.*, 1986; Miake *et al.*, 1990; Cuisinier *et al.*, 1992; Miake *et al.*, 1993; Ijima, Tohda & Moriwaki, 1992; Ijima, Tohda, Suzuki *et al.*, 1992; Iijima & Moriwaki, 1998; Bodier-Houllé *et al.*, 1998; Iijima & Moriwaki, 1999; Iijima *et al.*, 2001; Falini *et al.*, 2000).

The HA–OCP interface nucleation, orientation, morphology and assembly are, therefore, of great interest because they can be used to explain a very important component of some calcified tissue, and, for a long time, OCP

has been considered as a precursor of HA, the most biologically important phosphate, because of their close structural similarities (Falini *et al.*, 2000). For example, growth of HA on OCP is important to the understanding of the precipitation processes that occur during remineralization of artificial caries lesions in dental enamel.

Brown and co-workers (Brown, 1962; Brown *et al.*, 1962, 1979) first suggested a model for the HA–OCP interface in 1962, however, some considerations on the interface free energy were missing because their work was based on geometrical considerations. During the last decades many tools have been developed to study the atomic and electronic structures using both classical and quantum mechanics principles. These methods have helped in the structural determination and they have also shown how the experimental and analytical data can be used together in the crystal structure refinement and the corresponding electronic influence over the materials behavior. In this work we have performed the free-energy analysis of Brown's model and, from the resulting configuration after energy relaxation, we proposed a new model for the HA–OCP interface whose interfacial energy produces a more stable HA–OCP interface. High-resolution transmission electron microscopy (HREM) simulated images from our model show that this interface is quite smooth, but some misfit-dislocation-like features occur because of the unit-cell size.

2. Simulation method

Unit-cell models for HA and OCP were built according to the data determined by Kay *et al.* (1964) and Brown *et al.* (1962, 1979), respectively. In order to determine the electronic charge density of the HA and OCP, self-consistent field calculations were made using methods based on Density Functional Theory (DFT) with the Local Density Approximation (LDA) and the Generalized Gradient Approximation (GGA) developed by Perdew & Wang (1992), and using the *CASTEP* software (*Cerius*[2]; Molecular Simulations Inc., 1997). In all cases we consider a K-Points basis of 1 and consider 30 cycles and 50 steps by cycle. Electronic charge density (ECD) slice patterns were obtained at different directions and position values in the HA and OCP unit cells to identify the optimum matching of charge density iso-surfaces, to build interface configurations derived from the electronic interaction and not just from geometric rules.

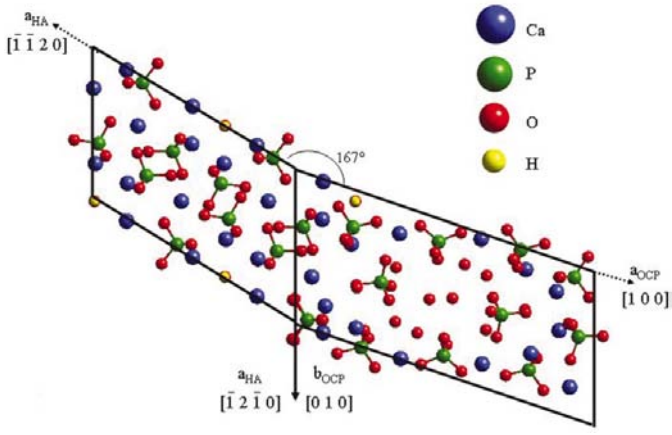

Figure 1
Brown's HA–OCP interface model. To create it, $[\bar{1}2\bar{1}0]_{HA}$ was 'glued' with $[010]_{OCP}$. Note that the c_{HA} axis is parallel to the c_{OCP} axis and that the angle between a_{HA} and a_{OCP} is 167°.

According to the results obtained, different models for the HA–OCP interface were proposed and evaluated, including that proposed by Brown *et al.* (1979). In the manipulation and interface building of the crystals, the *Cerius*[2] software (Molecular Simulations Inc., 1997) was used. The models were geometry optimized based on the minimal free energy using the 'Universal' potential to simulate the crystalline environment. Calculations by molecular and quantum mechanics were made for all the models built. ECD patterns were also obtained for the different HA–OCP interface models.

HREM images of the HA–OCP interface model with minimum free energy were calculated. The images were obtained by the multislice method with the *SimulaTEM* software developed by Gómez & Beltran del Rio (2001). The HREM images were obtained with a Jeol 200CX electron microscope: an accelerating voltage of 200 kV, a spherical aberration coefficient of $C_S = 1.2$ mm, a beam divergence half-angle of 0.5 mrad and a Scherzer resolution of 0.19 nm.

An experimental HREM image of the HA–OCP interface taken by Iijima, Tohda & Moriwaki (1992) (with the authors' authorization) was compared to the theoretically obtained images. The experimental image was digitally processed using *CRISP* software (Zou & Hovmöller, 1995), based on the periodicity of patterns in the Fast Fourier Transform (FFT), to enhance its contrast.

3. Results

Structurally there are some similarities between the unit cells of HA (Kay *et al.*, 1964; hexagonal $P6_3/m$, a = 9.418, c = 6.884 Å) and OCP (Brown, 1962; triclinic $P1$, a = 19.87, b = 9.63, c = 6.87 Å, α = 90.13, β = 92.13, γ = 108.36°) so it is not difficult to suggest how an HA–OCP interface can be built. Therefore, the unit-cell models for HA and OCP were obtained from the atomic positions determined by Kay *et al.* (1964) for HA and Brown *et al.* (1962, 1979) for OCP.

Brown's model of the HA–OCP interface was built in the way suggested (Brown, 1962; Brown *et al.*, 1962, 1979): the direction $[\bar{1}2\bar{1}0]$ of a half unit cell of HA was 'glued' with one unit cell of OCP along the direction [010]. In Fig. 1 the interface generated is shown along the c axis. Therefore, the relationship found for this model was: $[\bar{1}2\bar{1}0]_{HA}$ parallel to $[010]_{OCP}$ and $[0001]_{HA}$ parallel to $[001]_{OCP}$, and the angle between $[\bar{1}2\bar{1}0]_{HA}$ and $[010]_{OCP}$ was 167°.

After testing many possible interface configurations between these two crystals, in this work we propose a new HA–OCP interface model that was identified as the optimum. This was formed by half a unit cell of HA and one unit cell of OCP, as in Brown's model (Brown *et al.*, 1979), but in our case $[1\bar{2}10]$ of HA was 'glued' with [010] of OCP. Fig. 2 shows this

Table 1
Ca, P, O and H fractional atomic positions for the HA–OCP interface model proposed in this work.

The lattice parameters which refer to these atomic coordinates are a = 22.00, b = 9.63, c = 6.87 Å, α = 90.13, β = 92.13, γ = 108.36°; triclinic, $P1$.

Element	x	y	z
Ca	0.092	0.126	0.250
P	0.048	0.034	0.752
O	0.088	0.030	0.567
O	−0.066	0.429	0.750
O	0.092	0.033	0.930
O	0.030	0.575	0.750
O	0.006	0.163	0.756
O	−0.060	0.658	0.930
O	0.010	−0.100	0.756
P	−0.040	0.577	0.750
Ca	−0.064	0.253	0.999
Ca	−0.096	0.870	0.750
Ca	0.089	0.371	0.750
O	0.062	0.567	0.250
O	−0.035	0.421	0.250
O	0.056	0.338	0.430
P	0.036	0.419	0.250
Ca	0.060	0.743	0.499
O	−0.008	−0.152	0.250
O	−0.015	0.112	0.250
O	−0.092	−0.026	0.430
P	−0.051	−0.026	0.250
O	−0.142	0.228	0.250
Ca	−0.094	0.625	0.250
O	0.056	0.338	0.070
Ca	0.060	0.743	1.001
O	−0.092	−0.026	0.070
O	−0.060	0.658	0.570
Ca	−0.064	0.253	0.501
Ca	−0.064	0.253	−0.001
Ca	0.060	0.743	0.001
Ca	−0.096	−0.109	0.750

interface along the c axis. Therefore, in our model the a, b and c axes of HA are antiparallel to the a, b and c axes of OCP, respectively. The relationship found was: $[000\bar{1}]_{HA}$ parallel to $[001]_{OCP}$ and $[1\bar{2}10]_{HA}$ parallel to $[010]_{OCP}$, and the angle between $[1\bar{2}10]_{HA}$ and $[100]_{OCP}$ was 131°.

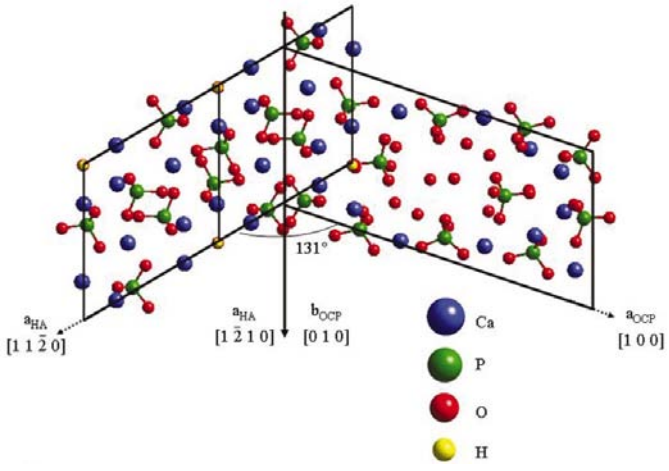

Figure 2
The HA–OCP interface model proposed in this work. To create it, $[\bar{1}2\bar{1}0]_{HA}$ was 'glued' with $[010]_{OCP}$. Note that in this case the $-c_{HA}$ axis is parallel to the c_{OCP} axis and that the angle between a_{HA} and a_{OCP} is 131°.

To use all the atomic positions of the models shown in Figs. 1 and 2 to calculate the energy relaxation is not possible because of the CPU capacity limits of the computer used. Thus, a triclinic $P1$ supercell of the interface was built with lattice parameters of a = 22.00, b = 9.63, c = 6.87 Å, α = 90.13, β = 92.13, γ = 108.36°. As can be seen, the parameters of the supercells used are similar to those of the OCP unit cell, with the exception of the doubling of the a axis to include more atoms. These supercells for Brown's model and for our model are shown in Figs. 3(a) and (c), respectively. Figs. 3(a) and (b) show the positions of the atoms in Brown's model before and after relaxation, and Figs. 3(c) and (d) shows those in the model proposed in this work. Note that in our model the positions of the atoms before and after relaxation are almost the same, but this is not the case for Brown's model. It is also worth mentioning that the atoms in Brown's model reached their positions of minimum energy after 16 relaxation steps, while our model reached it after 7 relaxation steps. The total energy of Brown's interface was −227886.15 eV and in our model it was −239776.70 eV. Table 1 shows the atomic positions in the above-mentioned supercell for the new proposed model of the HA–OCP interface after relaxation.

Fig. 4(a) shows the electronic charge density for the HA unit cell in the $(20\bar{2}0)$ plane along the $[10\bar{1}0]$ axis; the most external electron density contour (enhanced as a black contour) has a value of 0.5385 a.u. Fig. 4(b) shows the case for the OCP unit cell in the plane (100) along [100]; in this case the most external contour has a value of 0.5447 a.u. Note the environment produced by the electronic charge density around each atom and the arrangement they present both in HA and OCP unit cells. Fig. 5(a) shows the corresponding interface plane for Brown's model; here the most external contour has a value of 0.5624 a.u. Note in this figure that the environment of the atoms around the interface is not similar to that shown by the

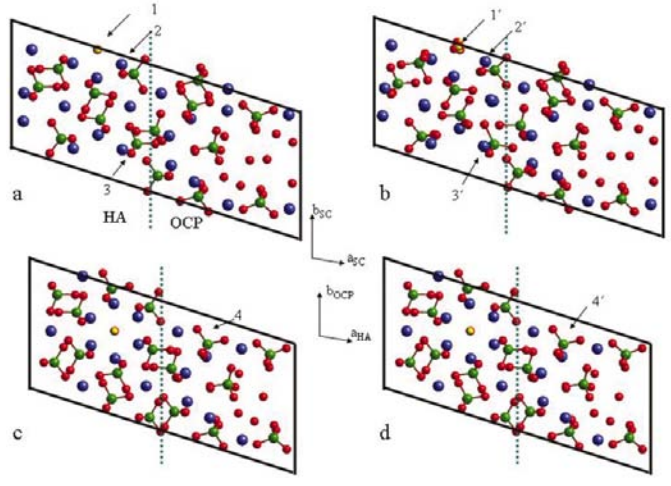

Figure 3
Projections of the super cells (SC) along [001] (a) and (c) before, and (b) and (d) after relaxation. (a) and (b) Brown's model; (c) and (d) the model proposed in this work. The dashed line indicates the interface position. Note that in our model the atom positions before and after relaxation (arrows No. 4) are almost the same, but they are not in Brown's model (arrows No. 1, 2 and 3).

Table 2
Distances for different atom bonds in the new proposed model for the HA–OCP interface before and after relaxation.

(*a*) P—O distances, (*b*) Ca—O distances and (*c*) O—H distances.

	Initial position	Final position		Initial position	Final position
(*a*) P—O					
1	1.5228	1.5044	10	1.5451	1.5225
1	1.5237	1.4750	10	1.5368	1.5217
1	1.5412	1.5113	10	1.5291	1.4826
1	1.5333	1.4670	10	1.5291	1.5302
2	1.5676	1.5030	11	1.5451	1.5244
2	1.5289	1.4868	11	1.5291	1.5000
2	1.5547	1.5064	11	1.5291	1.5112
2	1.5074	1.5751	11	1.5368	1.5405
3	1.5429	1.5396	12	1.5368	1.5040
3	1.5415	1.4756	12	1.5291	1.5178
3	1.5512	1.5478	12	1.5291	1.5333
3	1.554	1.5455	12	1.5451	1.4928
4	1.5204	1.5151	13	1.5451	1.4998
4	1.5455	1.5265	13	1.5368	1.5430
4	1.5141	1.4998	13	1.5291	1.5092
4	1.5666	1.5002	13	1.5291	1.5119
5	1.5109	1.5297	14	1.5451	1.5005
5	1.5521	1.5435	14	1.5291	1.5435
5	1.574	1.5129	14	1.5291	1.5116
5	1.5089	1.4950	14	1.5368	1.5166
6	1.5666	1.5145	15	1.5291	1.5545
6	1.5455	1.5118	15	1.5291	1.4911
6	1.5204	1.4949	15	1.5368	1.4929
6	1.5141	1.5072	15	1.5515	1.4973
7	1.5595	1.5282	16	1.5451	1.5038
7	1.5315	1.5395	16	1.5291	1.4958
7	1.538	1.4897	16	1.5291	1.5085
7	1.5565	1.5289	16	1.5368	1.4946
8	1.5291	1.4748	17	1.5291	1.5218
8	1.5291	1.4819	17	1.5291	1.5081
8	1.5451	1.5276	17	1.5451	1.4235
8	1.5368	1.5020	17	1.5368	1.5083
9	1.5451	1.4861			
9	1.5291	1.5168			
9	1.5291	1.5294			
9	1.5368	1.4833			

	Initial position	Final position
(*b*) Ca—O		
1	2.3444	2.3571
2	2.3444	2.3758
3	2.3444	2.413
4	2.3444	2.3402
5	2.3444	2.3378
6	2.3444	2.3427
7	2.2499	2.3027
8	2.3741	2.3965
9	2.3602	2.4302
10	2.3769	2.4023
11	2.5132	2.4769
12	2.4063	2.4873
(*c*) O—H		
1	0.9424	0.9372
2	0.9424	0.8799
3	0.9424	0.8103
4	0.9424	0.868

HA and OCP units cells in Fig. 4. Therefore, the electronic charge density results shown in Fig. 5(*a*) and its differences with Fig. 4 indicate that Brown's model is not the best model for the HA–OCP interface. Fig. 5(*b*) shows the charge density

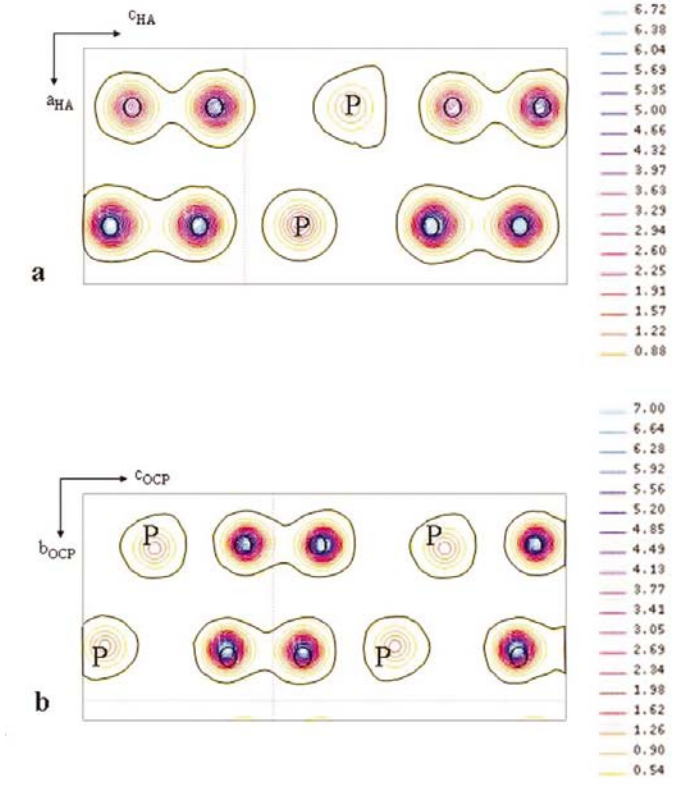

Figure 4
Electronic charge density patterns for (*a*) HA [plane (20$\bar{2}$0)] and (*b*) OCP [plane (100)] unit cells in the area of contact. Observe the charge distribution around each atom and compare it with those in Fig. 5. The most external contour is given in black for clarity.

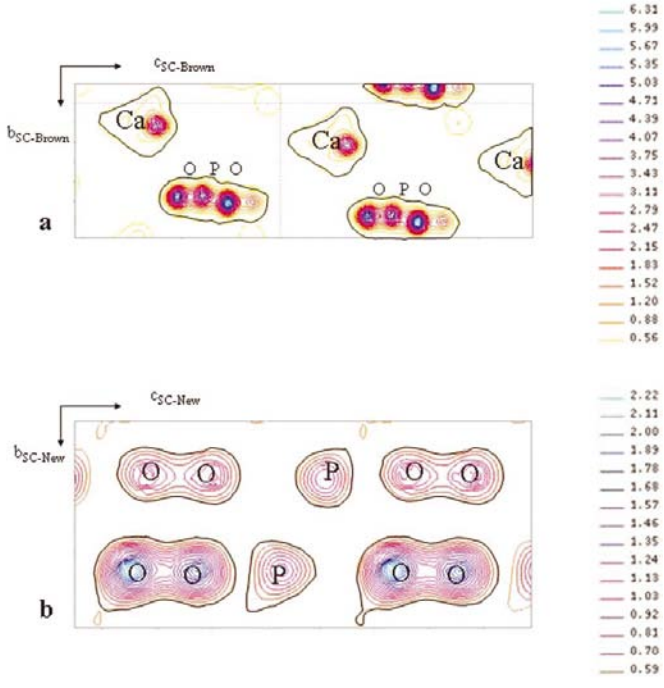

Figure 5
Electronic charge density patterns after relaxation of the supercells (SC) used and cut along the plane (900) for (*a*) Brown's interface model and (*b*) the interface model proposed in this work. The most external contour is given in black for clarity. Note the differences and similarities with the patterns shown in Fig. 4.

for our interface model; the most external contour has a value of 0.5972 a.u. In this case the electronic charge density distribution of the atoms around the interface is quite similar to those for HA and OCP unit cells.

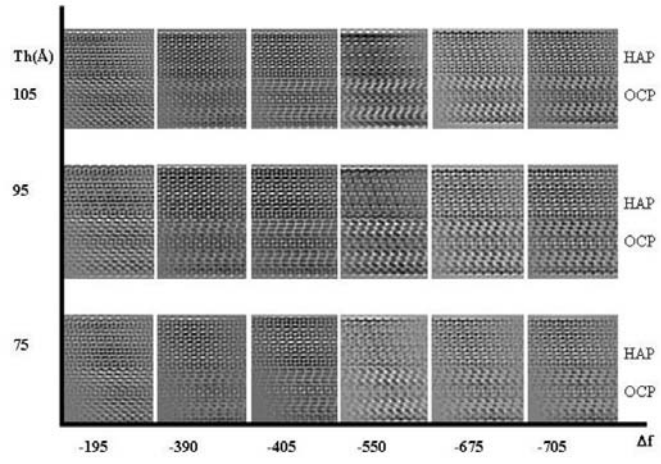

Figure 6
Series of simulated HREM images for the interface model proposed in this work for different thicknesses (Th) and defocus (Δf) values. The interface is shown along $[1\bar{2}13]_{HA}$ so that these images can be compared with the experimental image shown in Fig. 7.

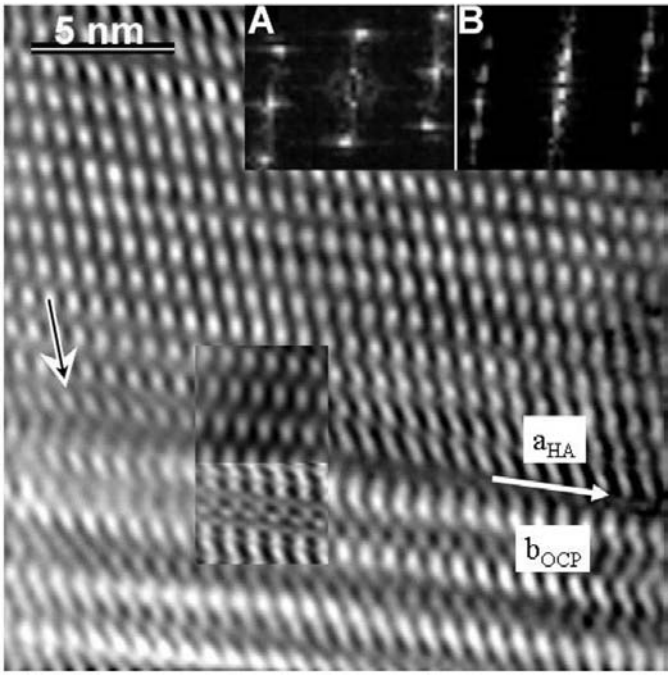

Figure 7
Experimental HREM image along the $[1\bar{2}13]_{HA}$ direction of the HA–OCP interface (Iijima, Tohda & Moriwaki, 1992), used with authorization from the authors). (*a*) Fourier transform from the HA zone; (*b*) Fourier transform from the OCP zone. The simulated HREM image with defocus $\Delta f = -550$ nm and thickness Th = 105 nm from Fig. 6 is shown in the inset. Looking at this image at a glance along the direction indicated by the arrow, a misfit-dislocation-like defect can be observed near the interface.

In the new proposed model we have analyzed the atom positions around the interface after relaxation, mainly the distances P—O, Ca—O and O—H, as resulted from Fig. 3(*d*). The P—O bond length reported in the literature is 1.63 Å (Huheey *et al.*, 1993). However, in the HA unit cell this distance varies from 1.52 to 1.54 Å; in OCP this length is in the range 1.51–1.57 Å. Our HA–OCP interface model shows, after relaxation, variations of the P—O distances in the range 1.47–1.54 Å. Similar distances for the P—O bond length have been reported in some simple inorganic compound structures of P and O such as P_4O_{10} and $[P_4O_{12}]^{4-}$ (Cartmell & Fowles, 1996). The distances for Ca—O and O—H reported in the literature (Huheey *et al.*, 1993) are 2.25 and 0.96 Å, respectively. In the HA unit cell this distance is 2.34 Å for Ca—O and 0.94 Å for O—H. In our model these distances, after relaxation, do not change considerably, and they are 2.33 and 0.93 Å for Ca—O and O—H, respectively. Table 2 shows the list for P—O, Ca—O, P—Ca and O—H bond lengths obtained in the interface from our model after relaxation. It is worth noting that in the optimization of the minimum free energy, the geometry of the system is adjusted in a variational way and the distances among atoms are ruled by the potential of the interaction. In our case, we used the potential named as 'Universal' in the program *Cerius*[2] and these distances are in agreement with those reported in the literature (Huheey *et al.*, 1993; Cartmell & Fowles, 1996).

Fig. 6 shows a defocus series for the HREM simulated image with different thicknesses along the $[1\bar{2}13]_{HA}$ axis

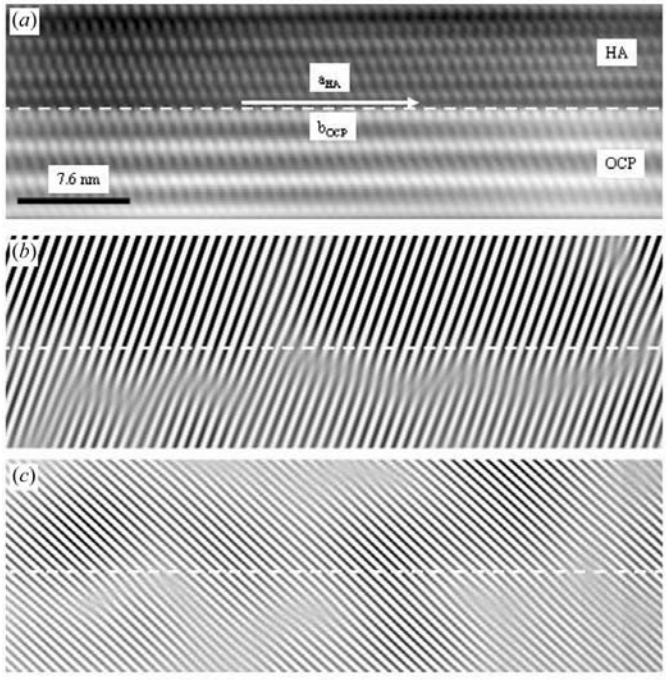

Figure 8
(*a*) Experimental HREM image of the HA–OCP interface taken from Iijima, Tohda & Moriwaki (1992) along the $[1\bar{2}13]_{HA}$ direction. (*b*) and (*c*) Processed images from (*a*); to obtain these images a filter that allowed the inclusion of (000) and one other reflection from the Fourier transform was used. Note the existence of some misfit-dislocation-like defects near the interface. The dashed line indicates the position of the interface.

obtained with the program *SimulaTEM* (Gómez & Beltran del Rio, 2001) for the HA–OCP interface model that we propose. This focal series was obtained along the $[1\bar{2}13]_{HA}$ axis to be able to compare it with the experimental image of the HA–OCP obtained by IIjima, Tohda & Moriwaki (1992). The experimental image was computer processed with the program *CRISP* (Zou & Hovmöller, 1995) to enhance its contrast (Fig. 7), and its Fourier transform shows that in this image HA is observed along the $[1\bar{2}13]$ direction. To check the existence (or not) of structural defects along the interface, the image was completely processed. If we took Fig. 7 at glance incidence along the direction indicated by the arrow, a dislocation-like feature is observed. Fig. 8 shows the result from image processing. These images were obtained with a filter that allowed the inclusion of the (000) transmitted reflection and one diffracted reflection from the Fourier transform producing lines along these directions. Note that in this case, the processed images show the existence of misfit-dislocation-like features. In fact, there is a zone of good fit followed by a zone of misfit. These misfit-dislocation-like features were also observed in the simulated image of the new model and they are produced by the difference that exists in their unit-cell parameters. Fig. 9(*a*) shows the simulated HREM image along the $[1\bar{2}13]$ direction for HA for the interface model proposed in this work, while Figs. 9(*b*) and (*c*) show the processed images obtained with similar filters than those used for Fig. 8. These processed images also present misfit-dislocation-like features close to the interface position.

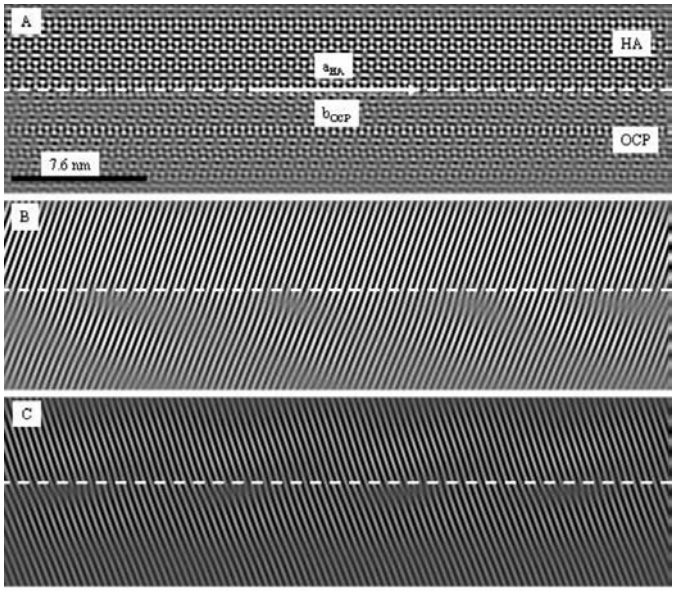

Figure 9
(*a*) Simulated HREM image of the HA–OCP interface from our model along the $[1\bar{2}13]_{HA}$ direction. (*b*) and (*c*) processed images from (*a*); they were obtained with a filter that allowed the inclusion of (000) and one other reflection from the Fourier transform. The dashed line indicates the position of the interface. Note the existence of misfit-dislocation-like defects near the interface.

4. Conclusions

In order to reproduce the experimentally reported epitaxic growth between HA and OCP, the interface was formed joining half a unit cell of HA and one cell of OCP, as indicated by Brown, but in such a way that $[000\bar{1}]_{HA}$ must be parallel to $[001]_{OCP}$ and $[1\bar{2}10]_{HA}$ is parallel to $[010]_{OCP}$. From the free energy analysis in Brown's model and in our model for the HA–OCP interface it was found that in Brown's model, after relaxation, the atoms around the interface do not have the same environment as they have in the HA and OCP unit cells, whereas in our interface model they do. The P—O, Ca—O and O—H distances in the zone around the interface were found in a reasonable range compared with those observed in the HA and OCP unit cells. All this indicates that our model is a better proposal for the study of the HA–OCP interface.

The HRTEM experimental image of the HA–OCP interface obtained by Iijima, Tohda & Moriwaki (1992) and the HREM simulated images obtained from our model show regions of good coherence in the interface separated by misfit-dislocation-like features. These structural defects are generated by the difference of 0.21 Å between a_{HA} and b_{OCP} unit-cell parameters. In the simulated image these defects are presented in a series whose periodicity is of approximately 10 nm.

The use of quantum mechanics calculations and the interpretation of electronic structure besides the symmetry of the crystal show a new way to determine the structure of interfaces, producing a model that must be considered in experimental studies. It is clear that Brown's model seemed adequate when the possibilities of understanding were limited to the geometry, however, with the newly developed tools, as with those used in this work, it is possible to include electronic parameters in the solution of the structure, producing a well supported HA–OCP interface model.

We thank L. Rendón, P. Mexia, C. Magaña, R. Hernández, J. Cañetas, S. Tehuacanero, M. Aguilar, and A. Sánchez for technical help. CONACYT and DGAPAUNAM (Projects PAPIIT IN103700 and IN104902) economically supported this work.

References

Bodier-Houllé, P., Steuer, P., Voegel, J. C. & Cuisinier, F. J. G. (1998). *Acta Cryst.* D**54**, 1377.
Brown, W. E. (1962). *Nature*, **196**, 1048–1050.
Brown, W. E., Schroeder, L. W. & Ferris, J. S. (1979). *J. Phys. Chem.* **83**, 1385–1388.
Brown, W. E., Smith, J. P., Lehr, J. R. & Frazier, A. W. (1962). *Nature*, **196**, 1050–1054.
Cartmell, E. & Fowles, G. W. A. (1996). *Valency and Molecular Structure*, pp. 184. London: Butterworths.
Cuisinier, F. J. G., Steuer, P., Senger, B., Voegel, J. C. & Frank, R. M. (1992). *Calcif. Tissue Int.* **51**, 259–268.
Falini, G., Gazzano, M. & Ripamonti, A. (2000). *J. Mater. Chem.* **10**, 535–538.
Gómez, A. & Beltran del Rio, L. (2001). *Rev. Latinoamericana Metal. Mater.* **21**, 46–50.

Huheey, J. E., Keiter, E. A. & Keiter, R. L. (1993). *Inorganic Chemistry Principles of Structure and Reactivity*, pp. 964. New York: Harper Collins College Publisher.
Iijima, M. & Moriwaki, Y. (1998). *J. Cryst. Growth*, **194**, 125–132.
Iijima, M. & Moriwaki, Y. (1999). *J. Cryst. Growth*, **198–199**, 670–676.
Iijima, M., Moriwaki, Y., Takagi, T. & Moradian-Oldak, J. (2001). *J. Cryst. Growth*, **222**, 615–626.
Ijima, M., Tohda, H. & Moriwaki, Y. (1992). *J. Cryst. Growth*, **116**, 319–326.
Ijima, M., Tohda, H., Suzuki, H., Yanagisawa, T. & Moriwaki, Y. (1992). *Calcif. Tissue Int.* **50**, 357–361.
Kay, M. I., Young, R. A. & Posner, A. S. (1964). *Nature*, **204**, 1050.
Mathew, M. & Takagi, S. (2001). *J. Res. Natl. Inst. Stand. Technol.* **106**, 1035–1044.
Miake, Y., Aoba, T., Moreno, E. C., Shimoda, S., Prostak, K. & Suga, S. (1990). *Calcif. Tissue Int.* **48**, 204–217.
Miake, Y., Shimoda, S., Fukae, M. & Aoba, T. (1993). *Calcif. Tissue Int.* **53**, 249–253.
Molecular Simulations Inc. (1997). *Cerius^{2}Molecular and Quantum Mechanics*. Molecular Simulation Inc., San Diego.
Nelson, D. G. A., Salimi, H. & Nancollas, G. H. (1986). *J. Colloid Interface Sci.* **110**, 32–39.
Perdew, J. P. & Wang, Y. (1992). *Phys. Rev. B*, **45**, 13244.
Rooji, J. F. & Nancollas, G. H. J. (1984). *Dent. Res.* **63**, 864.
Zou, X. & Hovmöller, S. (1995). *Electron Crystallography of Inorganic Structures. Theory and Practice*. Stockholm University Publications.